Regular Article

Simultaneous Voltammetric Measurement of Ascorbic Acid, Epinephrine, Uric Acid and Tyrosine at a Glassy Carbon Electrode Modified with Nanozeolite-Multiwall Carbon Nanotube

M. Noroozifar[a,]*, M. Khorasani-Motlagh[b], R. Akbari[a] and M. Bemanadi Parizi[a]

[a]*Analytical Research Laboratory, Department of Chemistry, University of Sistan and Baluchestan, Zahedan, P.O. Box 98155-147, Iran*

[b]*Inorganic Research Laboratory, Department of Chemistry, University of Sistan and Baluchestan, Zahedan, Iran*

In this study, incorporation of iron ion-doped natrolite nanozeolite, multi-wall carbon nanotubes into chitosan-coated glassy carbon electrode for the simultaneous determination of ascorbic acid, epinephrine, uric acid and tyrosine is studied. The results show that the combination of multi-wall carbon nanotubes and iron ion-doped natrolite zeolite causes a dramatic enhancement in the sensitivity of ascorbic acid, epinephrine, uric acid and tyrosine quantification. The sensor gave the separated and sharp voltammetric responses of analytes in four well-defined linear sweep voltammetry peaks. Under the optimum conditions, the calibration curve were linear up to 1.82×10^{-3}, 3.15×10^{-3}, 1.50×10^{-4} and 6.29×10^{-4} M with detection limits 1.82×10^{-6}, 1.33×10^{-6}, 4.09×10^{-8} and 2.01×10^{-7} M (S/N= 3) for ascorbic acid, epinephrine, uric acid and tyrosine, respectively. The analytical performance of this sensor has been evaluated for simultaneous detection of four analytes in human serum and urine samples.

INTRODUCTION

Ascorbic acid (AA) is an essential and a soluble vitamin widely present in many biological systems and is commonly used as an anti-oxidant for the prevention and treatment of the common cold and mental illness [1]. Besides, AA is a powerful anti-oxidant present in food and beverages, and it is also used as a marker chemical in evaluating food deterioration and product quality. It is also used for the prevention and treatment infertility, cancers, and AIDS (acquired immune deficiency syndrome) [2]. AA is necessary for the formation of collagen, which assists in the absorption of iron [3]. Epinephrine (Ep, 1-(3,4-dihydroxyphenyl)-2-methyloaminoethanol) is an important catecholamine neurotransmitter in the mammalian central nerves system [4,5]. Studies show that many diseases are related to the changes of Ep concentration. Therefore, it is important to examine its electrochemical behavior and to

develop a quantitative method for studying its physiological function in clinical medicine. Uric acid (UA) is the primary end product of purine metabolism, extreme level of UA in the body is symptoms of several diseases like gout, hyperuricaemia *etc*. Other diseases such as leukemia and pneumonia are also associated with enhanced urate level [6]. The normal UA level in serum range is from 240-520 µM and in urinary excretion is typically 1.4-4.4 mM [7]. Tyrosine (Tyr) is one of the most important amino acids which function as precursors of adrenaline, catecholamines, dopamine, and melanin. Parkinson's disease is generally found when tyrosine levels are abnormal [8]. Moreover, it is believed that several other disorders also are related to the metabolism of tyrosine, including atherosclerosis, lung diseases, liver diseases and mental illnesses.

In recent years, the development of voltammetric methods for simultaneous determination biomolecules in human fluid such as urine and serum has received considerable interest. AA, Ep, UA and Tyr play a crucial role in human metabolism. These compounds usually co-

---

*Corresponding author. E-mail: mnoroozifar@chem.usb.ac.ir

exist in the extra cellular fluid of the central nervous system and serum. Therefore, the individual or simultaneous determination of AA and co-existing species such as Ep, UA and Tyr is an important issue not only in diagnostic and pathological research but also in the field of biomedical chemistry. However, a major problem encountered is that biochemical compounds such as AA, Ep, UA and Tyr are oxidized at nearly same potential with poor sensitivity at unmodified electrodes. The overlap of their voltammetric responses makes their simultaneous determination highly difficult [9]. To overcome this problem, various modified electrodes have been constructed such as nanoparticles modified electrodes [10-13], hollow nitrogen-doped carbon microspheres pyrolyzed [14], organic redox mediators modified electrodes [15], boron-doped diamond electrode (BDD) [16], electrochemical oxidation in mild acidic media [17], polyacrylic acid-coated multi-wall carbon nanotubes [18], polymers modified electrodes [19-23], caffeic acid [24], carbon ceramic electrode [25], pyrolytic graphite electrode [26,27], screen-printed carbon electrode [28], carbon ionic liquid electrode [29], multi-wall carbon nanotube-poly(3,4-ethylendioxythiophene) (MWCNT-PEDOT) film [30] and carbon nanotube microelectrode [31].

Carbon nanotubes (CNTs) are excellent electrode materials due to their unique structure, good electrical conductivity, and mechanical strength. Also, zeolites are a group of hydrated aluminosilicates of different metals with a three-dimensional crystalline framework of tetrahedral silica or alumina anions strongly bonded at all corners, which contain channels filled with water and exchangeable cations. Also, adsorptive and ionic exchange properties of zeolite minerals were used as supporting materials for obtaining modified electrodes [32]. During the last two decades, zeolite modified electrodes (ZMEs) have been widely investigated, because of their chemical, physical and structural characteristics which make them of high interest in the design of electroanalytical systems [33,34]. Also, an interesting application of zeolite modified electrodes (ZMEs) is their use for the voltammetric detection of biochemical compounds [35]. Based on our best knowledge, there is no report on the application of modified GCE with iron ion-doped natrolite zeolite-multiwalled carbon nanotubes for the simultaneous determination of AA, Ep,

UA and Tyr. In this study, a new sensor for the simultaneous determination of AA, Ep, UA and Tyr using a combination of iron ion-doped natrolite zeolite as a modifier, multi-wall carbon nanotubes and chitosan as a binder is introduced. High sensitivity and selectivity, extraordinary stability, good reproducibility, technical simplicity, and noticeable ability of the proposed sensor to determine AA, Ep, UA and Tyr in real samples are the main advantages of the sensor. Thus, the proposed sensor can be of a significant attraction in biological research.

EXPERIMENTAL

Reagents and Materials

MWCNT with nanotube diameters, OD = 20-30 nm, wall thickness = 1-2 nm, length = 0.5-2 μm and purity of >95% was purchased from Aldrich. AA was purchased from Sigma-Aldrich and used as received. Ep, UA and Tyr were obtained from Merck and used as received. Chitosan ([2-amino-2-deoxy-(1-4)-β-D-glucopyranose]), a natural polymer, with medium molecular weight, 400000 Da, was purchased from Fluka and used without further purification. The natural natrolite (NA) zeolite was from Hormak region in Sistan & Baluchestan, Iran [36,37]. In order to prepare zeolite nanoparticles from natural NA (NANPs), a planetary ball mill (PM100, RETSCH Co.) was used. In dry milling stage, 50 g of zeolite was milled for 10 min at 500 rpm, and for wet milling, the resultant powder of the dry milling was mixed with 50 ml of water and milled for 3 h at 450 rpm. Acetic acid was diluted to a 1% aqueous solution before use. Due to the poor solubility of chitosan in water, its solution (2 mg ml^{-1}) was prepared in acetic acid solution. Appropriate amount of chitosan was mixed with 1% acetic acid solution and was stirred till complete dissolution of chitosan. The resulting solution was kept still overnight, and then was filtered through 0.22 m Millipore syringe filters to remove any impurity before use. To prepare buffer solutions with desired pHs, solutions of dichloroacetic acid (pK$_a$ = 1.26, for pH 1.0-1.8), chloroacetic acid (pK$_a$ = 2.87, for pH 1.8-3.8), acetic acid (pK$_a$ = 4.76, for pH 3.8-5.6) and KH$_2$PO$_4$ (for pHs 7.0-9.0) were prepared and their pHs were adjusted to the required values with sodium hydroxide solution. All solutions were prepared with doubly distilled

water. The electrolyte solutions were deoxygenated with nitrogen bubbling before each voltammetric experiment. All voltammetric experiments were performed under nitrogen atmosphere at room temperature.

Fresh urine and serum samples were obtained from the Omid Clinical Laboratory (Zahedan, Iran) and passed through a filter with suitable porosity.

Instrumentation

Electrochemical measurements were carried out with an SAMA500 Electroanalyser (SAMA Research Center, Iran) controlled by a personal computer. All electrochemical experiments were carried out in a conventional three-electrode cell at room temperature. A platinum electrode and a saturated calomel electrode (SCE) were used as the counter and reference electrodes, respectively.

TEM images were taken using a Philips CM120 transmission electron microscopy with resolution 2.5 Å. SEM image was taken using a Philips XL30 Scanning electron microscopy.

Preparation of Working Electrodes

The Na-form of the zeolitic material was prepared prior to modification. For this purpose the zeolitic material was agitated for 48 h in a 1 M NaCl solution at 25 °C, washed using distilled water until free of chloride ions ($AgNO_3$ test) and dried at 105 °C to constant weight. 1 g of Na-form of natrolite zeolite (Na-NAZ) was lightly ground and dispersed in 250 ml of a 0.01 M $(NH_4)_2Fe(SO_4)_2 \cdot 6H_2O$ solution under N_2 atmosphere and stirred for 48 h. The iron ion-doped natrolite (FeNAZ) was carefully washed with a HCl solution (pH 2) to remove occluded material and surface-adherent salt, and then washed with double distilled water till free of chloride ion and dried in air.

The optimum amount of FeNAZ (3 mg) was added to 3 mg MWCNTs and then 3 ml of chitosan 1% solution (CH) was added to this mixture and the resulting mixture was dispersed with the help of ultrasonic agitation for 2 h to form a FeNAZ-MWCNT-CH suspension. The glassy carbon (GC) working electrode with 3 mm of diameter (0.0706 cm^2) was polished with 0.05 μm alumina slurry to a mirror-finish. After rinsing with double-distilled water, it was sonicated in water and absolute ethanol for about 5 min. Then for more cleaning and activation of the GC electrode,

it was immersed into a freshly prepared deoxygenated 1.0 M H_2SO_4 and cyclic scans were performed in the potential range of -1.5 and +1.5 V at a scan rate of 100 mV s^{-1} until a stable cyclic voltammetric profile (≈ 15 times) was obtained. The clean GC electrode was coated by casting 5.0 μl of the FeNAZ-MWCNT-CH suspension and dried under infrared radiation. This modified GC electrode was denoted as GC/FeNAZ-MWCNT-CH. When not in use, the modified electrode was stored in DDW. Also, the GC/NAZ-MWCNT-CH without Fe and GC/MWCNT-CH were prepared with the same method.

RESULTS AND DISCUSSION

SEM and TEM Characterization

Surface morphology of the zeolite sample was investigated using SEM. SEM image of the zeolite (Fig. 1A) revealed the uniform shape of the zeolite granules. Figure 1B shows the TEM images of prepared FeNAZ-MWCNT. It can be seen that MWCNTs and FeNAZ is heavily entangled with one another. For comparison, a FeNAZ-MWCNT-CH was made (Fig. 1C). However, in the presence of CH, the MWCNTs and FeNAZ are not so aggregate. The probable reason is that CH as a natural polymer can interact with MWCNTs and makes the heavily entangled MWCNT bundles from finer bundles [38].

Electrochemical Characteristics of Modified Electrode

According to the detection principle, any cation small enough to enter the natrolite structure is theoretically able to liberate Fe species by ion exchange and, therefore, to give a corresponding amperometric signal. Figure 2A shows the cyclic voltammograms (CVs) of the modified electrode obtained in dichloroacetic acid buffer solution (DCAAB) with pH = 1.0. The voltammogram of FeNAZ-MWCNT-CH exhibited a pair of redox peaks with a formal potential of 0.23V *vs*. SCE, and potential peak separation $\Delta E_p = 0.1$ V which can be attributed to the electron transfer between Fe(II) and Fe(III) in the FeNAZ.

As shown in Fig. 2B, I_{pa} and I_{pc} are linearly dependent on scan rate, as expected for surface confined redox process. Moreover, the ratio of the anodic peak current to the cathodic peak current, I_{pa}: I_{pc}, is almost equal to unity. These
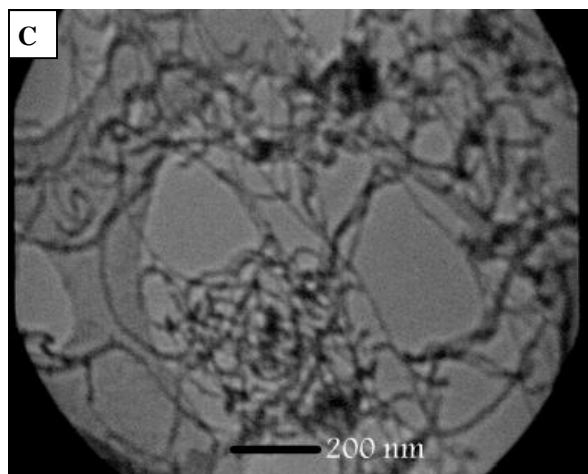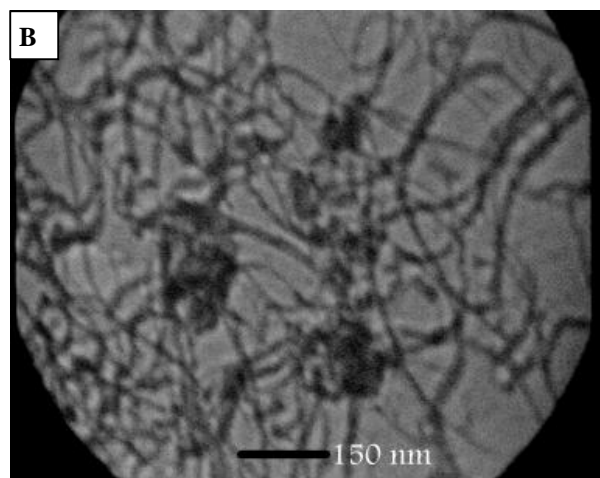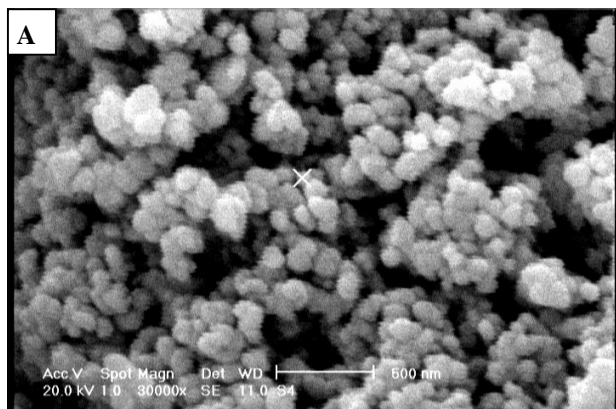
Fig. 1. (A) SEM image of the Natrolite zeolite (B) TEM images of prepared FeNAZ-MWCNT and (C) TEM image of the FeNAZ-MWCNT-CH.
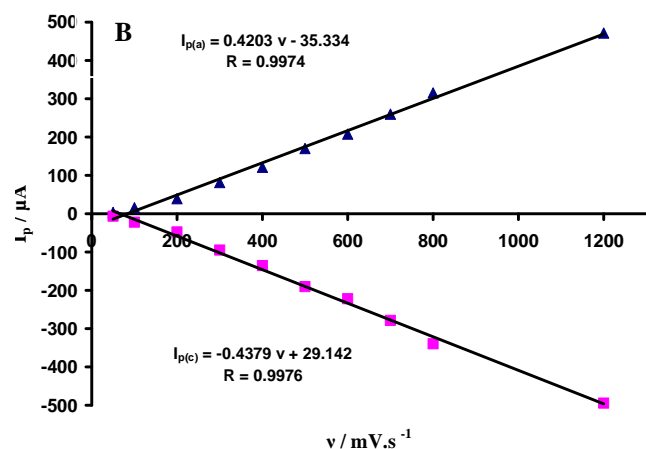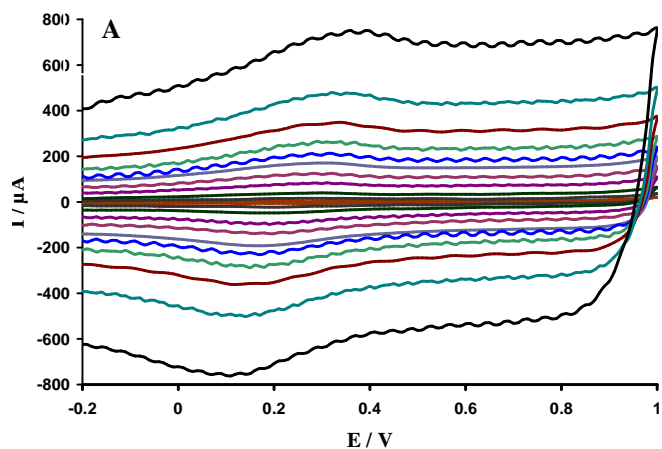

Fig. 2. Cyclic voltammograms of GC/FeNAZ-MWCNT-CH electrode in DCAABS (pH 1) at various scan rates (from inner to outer curve): 50, 100, 200, 300, 400, 500, 600, 700, 800 and 1200 mV s^{-1};B) the plot of peak currents *vs*. scan rates.

behaviors are consistent with a surface confined [39] quasi-reversible electron transfer process.

Electrocatalytic Oxidation of AA, Ep, UA and Tyr

Figure 3A displays the LSVs of a quaternary mixture of AA, Ep, UA and Tyr in 0.1 M DCAAB solution (pH 1.0) at bare GC (BGC), GC/MWCNT-CH, GC/NAZ-MWCNT-CH, and GC/FeNAZ-MWCNT-CH modified electrodes. BGC electrode showed weak oxidation peaks for AA, a broad overlapped oxidation peak for Ep-UA and a broad
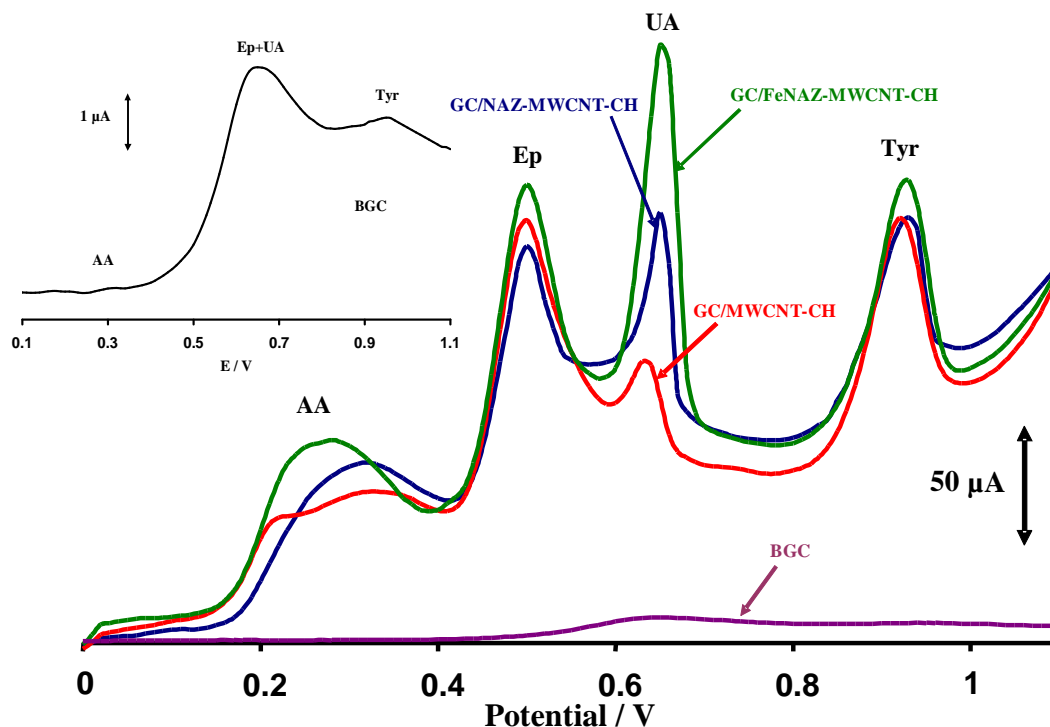
Fig. 3. LSVs behaviors of a mixture of AA, Ep, UA and Tyr (46.0×10^{-5}, 56.5×10^{-5}, 75×10^{-6} and 16.0×10^{-5} M, respectively) at the surface of BGC, GC/MWCNT-CH, GC/NAZ-MWCNT-CH and GC/FeNAZ-MWCNT -CH electrodes in 0.1 M DCAABS (pH 1) at the scan rate of 100 mV s^{-1}.

peak for Tyr at 0.32, 0.65 and 0.96 V, respectively. It is difficult to locate the oxidation potential of Ep and UA from Fig. 3 by using BGC electrode. It has been almost merged with the oxidation potential of Tyr. Further, in the subsequent cycles, the oxidation peak of AA were shifted to the positive potential and after 10 cycles, oxidation peaks were observed for them at 0.38 V. The oxidation peak of Try has been also merged with oxidation peak of Ep-UA with decreased peak current of oxidation peak of Ep-Tyr. This revealed that bare GC electrode is not suitable for the stable determination of AA, Ep, UA and Tyr.

Modified electrodes oxidized AA, Ep, UA and Tyr in four well-defined LSV peaks with enhanced oxidation current response increase as follow: GC/FeNAZ-MWCNT-CH>GC/NAZ-MWCNT-CH>GC/MWCNT-CH. Further, the oxidation peaks of AA, Ep, UA and Tyr are more stable at GC/FeNAZ-MWCNT-CH modified electrode in the subsequent cycles. The separations of oxidation peak potentials of AA-Ep, Ep-UA and UA-Tyr at GC/FeNAZ-

MWCNT-CH modified electrode are of 260 mV, 150 mV and 280 mV, respectively, which were enough for the simultaneous determination of this quaternary mixture.

In contrast to BGC electrode, when GC/MWCNT-CH, GC/NAZ-MWCNT-CH or GC/FeNAZ-MWCNT-CH were used as working electrodes, the detection sensitivity was improved significantly and effective separation of the anodic peaks of AA, Ep, UA and Tyr was obtained (Fig. 3). The large peak separation of the anodic peaks for these four compounds allows us to simultaneously determine them in the mixture solutions. Also, Fig. 3 compares the catalytic effect of MWCNT-CH, NAZ-MWCNT-CH and FeNAZ-MWCNT-CH for detection of these compounds. It can be seen from Fig. 3, that FeNAZ-MWCNT-CH has more electrocatalytic effect toward the oxidation of AA, Ep, UA and Tyr. This phenomenon could be explained by considering that the cation exchange character of the zeolite modifier leads to an uptake of the cationic tyrosine in acidic media. The same result has been reported by Wang and

Walcarius [40]. The LSVs of AA, Ep, UA and Tyr at GC/FeNAZ-MWCNT-CH showed excellent improvement in the oxidation peak currents for AA, Ep, UA and Tyr. There are some reports on the tendency of complex formation between iron ions and AA [41] and UA [42]. Therefore, AA, UA and Tyr as well as Ep could be more accumulated on the electrode surface due to their interaction with iron ions. Consequently, application of the GC/FeNAZ-MWCNT-CH leads to the enhancement of current sensitivity and selectivity in simultaneous determinations of AA, Ep, UA and Tyr. Also, the results in Fig. 3 clearly showed that the electrochemical responses of AA, Ep, UA and Tyr on the FeNAZ-MWCNT-CH electrode have occurred at different potential windows, which means that the electrochemistry of these four compounds can be well resolved from their mixed solutions. The results indicate that the oxidation peak potential for these analytes is close to each other on BGC. But, the enhancements of the anodic peak currents for AA, Ep, UA and Tyr are most predominant at GC/FeNAZ-MWCNT-CH than those at other electrodes.

Effect of pH on the Oxidation of AA, Ep, UA and Tyr

The effect of solution pH on the electrochemical response of the GC/FeNAZ-MWCNT-CH towards the simultaneous determination of AA, Ep, UA and Tyr was studied in the pH range from 1.0 to 7.0 Based on the results, the anodic peak current of AA and Tyr increases with an increase in the solution pH until it reaches to 3.0 and then the anodic peak current of AA and Tyr decreases with increasing pH until pH 7.0. The anodic peak current of Ep and UA decreases slightly with an increase in the solution pH until pH 4.0 and then the anodic peak current of Ep increases with increasing pH until pH 7.0 but, the anodic peak current of UA decreases with increasing pH until pH 7.0. In addition, all the anodic peak potentials for the oxidation of AA, Ep, UA and Tyr were decreased linearly with increasing pH from 1.0 to 7.0, showing that protons have taken part in their electrode processes. Figure 4 shows the CVs of AA, DA and UA in various pHs. It was found that the anodic peak potentials for AA, Ep, UA and Tyr shift to negative potentials by increasing pH. This was expected because of the participation of proton(s) in the oxidation
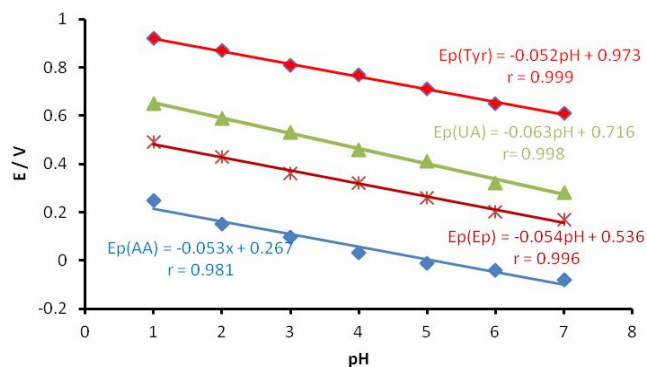

Fig. 4. Influence of supporting electrolyte pH on peak potentials of AA, Ep, UA and Tyr at GC/FeNAZ-MWCNT-CH electrode.

reactions of AA, Ep, UA and Tyr. The oxidation reaction can be explained as follows

$$R - mH^+ - ne \rightleftharpoons O \qquad (1)$$

where, R stands for AA, Ep, UA and Tyr; O stands for the responding products; m and n are the number of protons and electrons involved in the reaction. The anodic peak potentials are given by [43]:

$$E'_{p(R)} = E_{p(R, pH = 0)} - \frac{2.303mRT}{nF} pH \qquad (2)$$

where $E_{p(R, pH = 0)}$ is the anodic peak potential for Red at pH = 0.0, and R, T, and F have their usual meanings. The values of $E_{p(R)}$ are plotted in Fig. 4. As can be seen in Fig. 4, $E'_{p(Red)}$ were shifted to negative potentials with the slopes of 0.053, 0.054, 0.060 and 0.052 V/pH for AA, Ep, UA and Tyr, respectively, which are in agreement with the theoretical slope ($-2.303mRT/nF$) of 0.059 (m/n)V/pH. These results suggest that oxidation of AA, Ep, UA and Tyr involves an equal number of protons and electrons (m = n) [44].

Also, it must be noted, that from pH 1.0 to higher pH the anodic peak potentials of Ep and UA were broader and overlapped together. Because of having better peaks separation and satisfactory peak currents, a DCAAB buffer

solution with pH 1.0 was chosen as optimal pH.

Effect of Scan Rate

The cyclic voltammograms of the GC/FeNAZ-MWCNT-CH in DCAAB solution at pH 1.0 in present of AA, Ep, UA and Tyr were recorded at various scan (Fig. 5A). There is a linear correlation between the cathodic current and $v^{1/2}$, suggesting that the kinetics of the overall process are controlled by mass transport of AA, Ep, UA and Tyr from the bulk solution to the electrode surface; however, at higher scan rates, some deviation from linearity is observed (Fig. 5B). It is noteworthy that the anodic oxidation (or reduction for Ep) peak potential, E_p, for AA, Ep, UA and Tyr shifted slightly to more positive (or negative for reduction of Ep) potentials with increasing scan rate. These results indicated that a kinetic limitation exists in the course of reaction between the FeNAZ-MWCNT-CH composite and AA, Ep, UA and Tyr, at higher scan rates.

Interference

The electro-oxidation processes of AA, Ep, UA and Tyr at the GC/FeNAZ-MWCNT-CH in the mixture have been also investigated when the concentration of one species changed, whereas those of other two species were kept constant (Fig. 6).

Examination of Fig. 6A showed that the peak current of AA is increased with an increase in AA concentration when the concentrations of Ep, UA and Tyr were kept constant. Although the charge current was enhanced after AA was oxidized, the peak currents of Ep, UA and Tyr did not change. Similarly and obviously, as shown in Fig. 6B, C and D, keeping the concentrations of other three compounds constant, the oxidation peak currents of Ep, UA and Tyr were positively proportional to their concentration, while those of other three compounds did not change.

Calibration Curve

From our experimental results described above, it was known that in the quaternary mixture containing AA, Ep, UA and Tyr, when a GC/FeNAZ-MWCNT-CH was used the oxidation peaks of these four compounds were clearly separated from each other, but when the other modified electrodes were used as working electrodes these species could not be determined simultaneously. If the
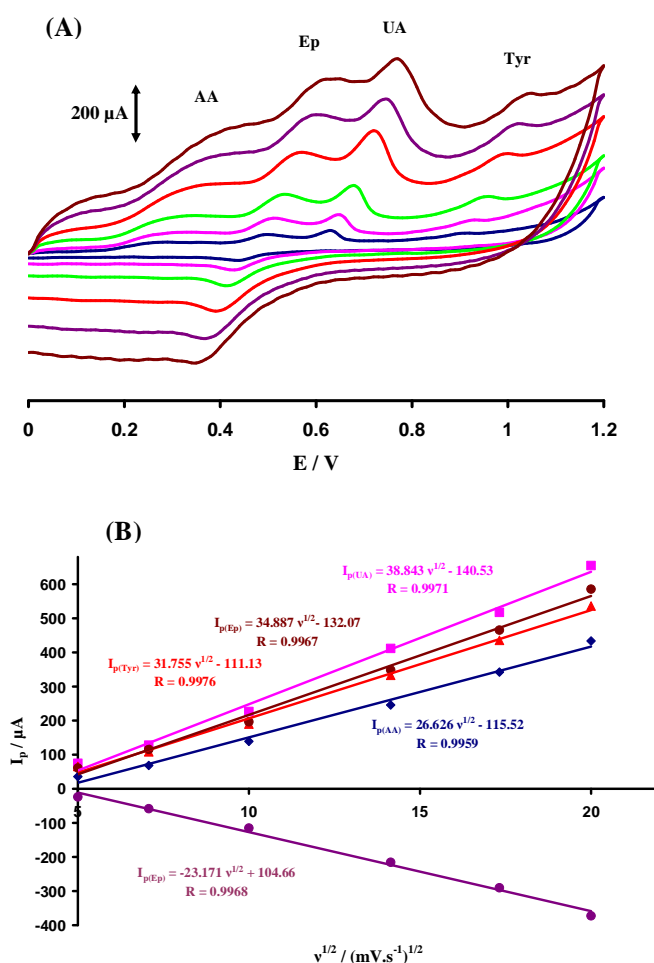

(A)

(B)

Fig. 5. A) CVs of a mixture of AA, Ep, UA and Tyr (85.0×10^{-5}, 60.0×10^{-5}, 70×10^{-6} and 15.5×10^{-5} M, respectively) at different scan rates (from inner to outer curve): 25, 50, 100, 200, 300 and 400 mV s^{-1}. B) the plots of I_p for each analyte *vs.* $v^{1/2}$.

concentrations of AA, Ep, UA and Tyr increased synchronously, on increasing the concentrations of the four compounds, the peak currents at the GC/FeNAZ-MWCNT-CH electrode increase accordingly. A sample LSVs of a quaternary mixture of AA, Ep, UA and Tyr is shown in Fig. 7.

Using the experimental conditions described above, the calibration curve are linear in the range of 5.00×10^{-6}-1.82×10^{-3}, 4.50×10^{-6}-3.15×10^{-3}, 5.00×10^{-7}-1.50×10^{-4} and 5.50×10^{-7}-6.29×10^{-4} M for AA, Ep, UA and Tyr, respectively. Also, the theoretical detection limits, based on
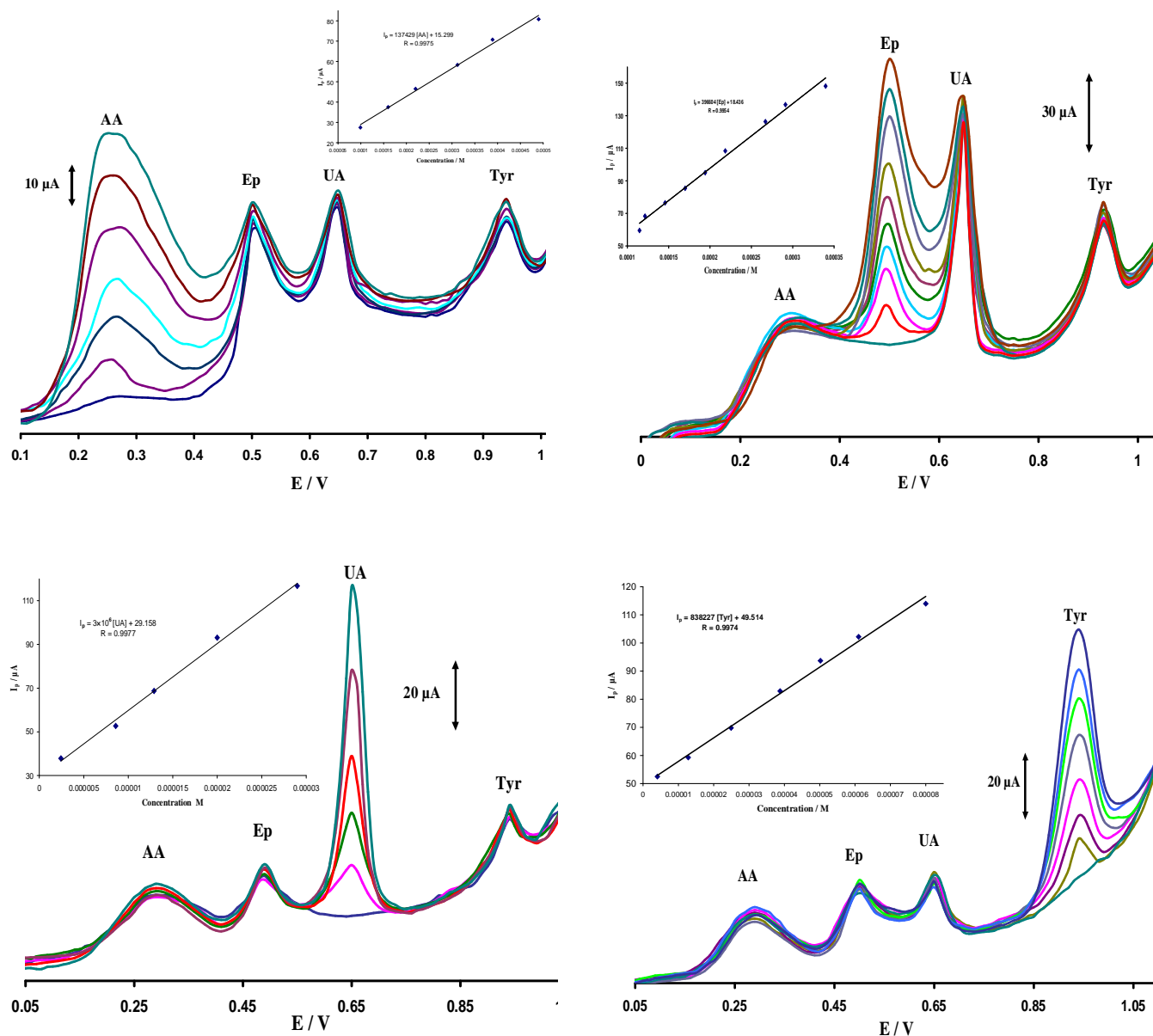
Fig. 6. LSVs for the mixture containing AA, Ep, UA and Tyr with different concentrations in DCAABS (pH 1.0) at the GC/FeNAZ-MWCNT-CH modified electrode. (A) Ep (15.0×10^{-5} M), UA (13.0×10^{-6} M), Tyr (17.0×10^{-6} M) and AA (a-f: 0.0, 9.9×10^{-5}, 16.0×10^{-5}, 22.0×10^{-4}, 31.2×10^{-5}, 38.9×10^{-5} and 49.0×10^{-5} M); (B) AA (24.0×10^{-5} M), UA (34.0×10^{-6} M), Tyr (45.0×10^{-6} M) and Ep (a-j: 0.0, 11.4×10^{-5}, 12.1×10^{-5}, 14.5×10^{-5}, 16.9×10^{-5}, 19.4×10^{-5}, 21.8×10^{-5}, 26.6×10^{-5}, 29.1×10^{-5} and 33.9×10^{-5} M); (C) AA (12.5×10^{-5} M), Ep (6.2×10^{-5} M), Tyr (4.0×10^{-6} M) and UA (a-f: 0.0, 2.4×10^{-6}, 8.6×10^{-6}, 12.9×10^{-6}, 20.0×10^{-6} and 29.0×10^{-6} M) ; AA (11.0×10^{-5} M), Ep (6.5×10^{-5} M), UA (3.5×10^{-6} M) and Tyr (a-h: 0.0, 4.0×10^{-6}, 12.8×10^{-6}, 24.9×10^{-6}, 38.8×10^{-6}, 50.2×10^{-6}, 61.0×10^{-6} and 80.0×10^{-6} M).
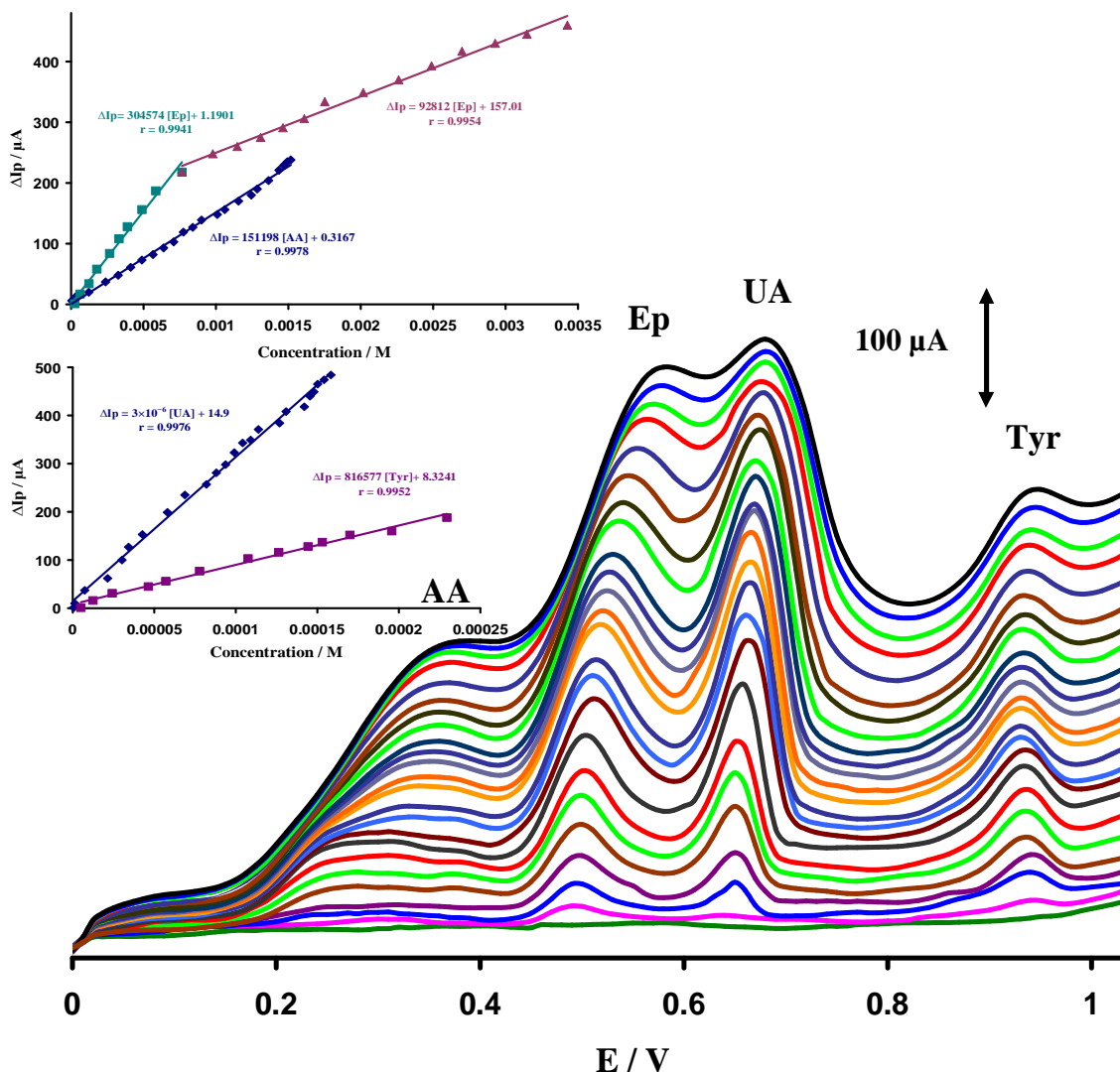
Fig. 7. A sample LSVs of the mixtures of AA, Ep, UA and Tyr at the surface of GC/FeNAZ-MWCNT-CH electrode in DCAABS (pH 1.0) at the scan rate of 100 mV s^{-1}. concentrations from inner to outer of curves : AA (0.0, 5.0×10^{-6}, 3.72×10^{-5}, 12.4×10^{-5}, 23.7×10^{-5}, 32.5×10^{-5}, 41.1×10^{-5}, 48.9×10^{-5}, 56.5×10^{-5}, 63.8×10^{-5}, 70.8×10^{-5}, 77.5×10^{-5}, 84.0×10^{-5}, 90.0×10^{-5}, 10.1×10^{-4}, 10.6×10^{-4}, 11.55×10^{-4}, 12.4×10^{-4}, 12.8×10^{-4}, 13.6×10^{-4}, 14.3×10^{-4}, 14.6×10^{-4}, 14.9×10^{-4} and 15.1×10^{-4} M), Ep (0.0, 2.5×10^{-5}, 6.2×10^{-5}, 12.3×10^{-5}, 17.8×10^{-5}, 26.6×10^{-5}, 33.1×10^{-5}, 38.9×10^{-5}, 48.9×10^{-5}, 58.5×10^{-5}, 76.5×10^{-5}, 97.8×10^{-5}, 11.5×10^{-4}, 13.1×10^{-4}, 14.6×10^{-4}, 16.1×10^{-4}, 17.5×10^{-4}, 20.1×10^{-4}, 22.6×10^{-4}, 24.9×10^{-4}, 27.0×10^{-4}, 29.2×10^{-4}, 31.4×10^{-4} and 34.3×10^{-4} M), UA (0.0, 5.0×10^{-7}, 1.2×10^{-6}, 7.3×10^{-6}, 21.3×10^{-6}, 30.1×10^{-6}, 34.2×10^{-6}, 42.7×10^{-6}, 58.0×10^{-6}, 68.7×10^{-6}, 88.0×10^{-6}, 93.7×10^{-6}, 99.0×10^{-6}, 10.4×10^{-5}, 10.9×10^{-5}, 11.4×10^{-5}, 12.7×10^{-5}, 13.1×10^{-5}, 14.2×10^{-5}, 14.5×10^{-5}, 14.7×10^{-5}, 15.0×10^{-5}, 15.4×10^{-5} and 15.8×10^{-5} M) and Tyr (0.0, 5.0×10^{-6}, 12.4×10^{-6}, 24.2×10^{-6}, 46.4×10^{-6}, 57.0×10^{-6}, 77.7×10^{-6}, 10.7×10^{-5}, 12.6×10^{-5}, 14.4×10^{-5}, 15.3×10^{-5}, 17.0×10^{-5}, 19.5×10^{-5}, 22.9×10^{-5}, 26.2×10^{-5}, 29.2×10^{-5}, 35.0×10^{-5}, 40.3×10^{-5}, 42.8×10^{-5}, 49.7×10^{-5}, 53.9×10^{-5}, 58.5×10^{-5}, 62.9×10^{-5} and 73.0×10^{-5} M). Inset: the calibration curves for analytes.

Table 1. Determination of AA, Ep, UA and Tyr in Human Serum and Urine Samples Using GC/FeNAZ-MWCNT-CH

Sample	Analyte	Detected (μM)	Added (μM)	Found (μM)	Recovery (%)	RSD (%)
	AA	-	30	29.2	97.3	1.5
Serum 1	Ep	-	50	51.4	102.8	0.9
	UA	9.5	50	60.1	101.0	1.6
	Tyr	6.2	25	32.5	104.1	2.2
	AA	-	25	24.1	96.4	2.6
Serum 2	Ep	-	70	71.8	102.5	1.2
	UA	17.9	25	43.5	101.3	0.8
	Tyr	7.4	50	59.5	103.6	1.9
	AA	-	25	24.5	98.0	1.3
Urine 1	Ep	-	75	76.3	101.7	2.4
	UA	48.4	50	102.9	104.5	1.4
	Tyr	25.2	50	79.9	106.2	2.3
	AA	-	50	49.2	98.4	1.8
Urine 2	Ep	-	50	50.9	101.8	2.2
	UA	61.7	40	106.9	105.1	1.8
	Tyr	52.7	50	104.8	102.0	2.8

3σ, of the proposed method were 1.82×10^{-6}, 1.33×10^{-6}, 4.09×10^{-8} and 2.01×10^{-7} M for AA, Ep, UA and Tyr, respectively.

Real Samples

Human serum and urine samples were selected as real samples for analysis by the proposed method using the standard addition method. To avoid the interferences of the real samples matrix, and to fit into the linear range of AA, Ep, UA and Tyr, only 0.5 ml of urine and serum samples were added to the electrochemical cell containing 5.0 ml of DCAAB (pH 1.0) solution. To ascertain the correctness of the results, the diluted sample mentioned above was spiked with certain amounts of AA, Ep, UA and Tyr and then was detected. The recovery of the spiked samples ranged between 96.4 and 105.1% (Table 1).

CONCLUSIONS

The modification of the GC electrode surface by FeNAZ-MWCNT-CH not only improves the electrochemical

catalytic activities towards the oxidation of AA, Ep, UA and Tyr, but also resolves the overlapped oxidation peaks of AA, Ep, UA and Tyr into four well-defined peaks at potentials 0.24 V, 0.50V, 0.65 and 0.93V in LSV, respectively. Comparison between GC/MWCNT and GC/NAZ-MWCNT-CH demonstrates that GC/FeNAZ-MWCNT-CH facilitates more the simultaneous determination of AA, Ep, UA and Tyr with good stability, sensitivity and selectivity.

In comparison with other electroanalytical methods reported for the simultaneous determination of AA, Ep, UA and Tyr, this method has better figures of merit. The proposed method can be applied to the simultaneous determination of AA, Ep, UA and Tyr concentrations in real samples with satisfactory results.

ACKNOWLEDGMENTS

REFERENCES

[1] M.R. Moghadam, S. Dadfarnia, A.M. Haji Shabani, P. Shahbazikhah, Anal. Biochem. 410 (2011) 289.

[2] M.B. Davies, J. Austin, S.A. Partridge, Vitamin C: Its Chemistry and Biochemistry, Royal Society of Chemistry, Cambridge, UK, 1991.

[3] A.B. Florou, M.I. Prodromidis, M.I. Karayannis, S.M. Tzouwara-Karayanni, Anal. Chim. Acta 409 (2000) 113.

[4] Y. Zeng, J. Yang, K. Wu, Electrochim. Acta 53 (2008) 4615.

[5] S. Shahrokhian, M. Ghalkhani, M.K. Amini, Sens. Actuators B 137 (2009) 669.

[6] G.G. Guilbault, Analytical Uses of Immobilised Enzymes. Marcel Dekker, New York, 1984.

[7] P.T. Kissinger, L.A. Pachla, L.D. Reynolds, S. Wright, J. Assoc. Anal. Chem. 70 (1987) 1.

[8] W. Wei, W. Hong-Jian, J. Chong-Qiu, S. Jing-Min, Chin. J. Anal. Chem. 35 (2007) 1772.

[9] R.D. O'Neil, Analyst 119 (1994) 767.

[10] M. Noroozifar, M. Khorasani-Motlagh, A. Taheri, Talanta 80 (2010) 1657.

[11] S. Thiagarajan, S.M. Chen, Talanta 74 (2007) 212.

[12] J.S. Huang, Y. Liu, H.Q. Hou, T.Y. You, Biosens. Bioelectron. 24 (2008) 632.

[13] J. Weng, J.M. Xue, J. Wang, J.S. Ye, H.F. Cui, F.S. Sheu, Q.Q. Zhang, Adv. Funct. Mater. 15 (2005) 639.

[14] C. Xiao, X. Chu, Y. Yang, X. Li, X. Zhang, J. Chen, Biosens. Bioelectron. 26 (2011) 2934.

[15] H.R. Zare, N. Nasirizadeh, M. Mazloum Ardakani, J. Electroanal. Chem. 577 (2005) 25.

[16] P.S. Siew, K.P. Loh, W.C. Poh, H. Zhang, Relat. Mater. 14 (2005) 426.

[17] S. Thiagarajan, T.H. Tsai, S.M. Chen, Biosens. Bioelectron. 24 (2009) 2712.

[18] S.-H. Huang, H.-H. Liao, D.-H. Chen, Biosens. Bioelectron. 25 (2010) 2351.

[19] L.Q. Lin, J.H. Chen, H. Yao, Y.Z. Chen, Y.J. Zheng, X.H. Lin, Bioelectrochem. 73 (2008) 11.

[20] O. Niwa, M. Morita, H. Tabei, Electroanalysis 6 (1994) 237.

[21] H.R. Zare, N. Rajabzadeh, N. Nasirizadeh, M. Mazloum Ardakani, J. Electroanal. Chem. 589 (2006) 60.

[22] Z.Q. Gao, H. Huang, Chem. Commun. (1998) 2107.

[23] Y.X. Li, X.Q. Lin, Sens. Actuator B 115 (2006) 134.

[24] W. Ren, H. Q. Luo, N. B. Li, Biosens. Bioelectron. 21 (2006) 1086.

[25] A. Salimi, H. Mam-Khezri, R. Hallaj, Talanta 70 (2006) 823.

[26] [26] R.P. Silva, A.W.O. Lima, S.H.P. Serrano, Anal. Chim. Acta 612 (2008) 89.

[27] R.T. Kachoosangi, R.G. Compton, Anal. Bioanal. Chem. 387 (2007) 2793.

[28] K.S. Prasad, G. Muthuraman, J.M. Zen, Electrochem. Commun. 10 (2008) 559.

[29] A. Safavi, N. Maleki, O. Moradlou, F. Tajabadi, Anal. Biochem. 359 (2006) 224.

[30] K.-C. Lin, T.-H. Tsai, S.-M. Chen, Biosens. Bioelectron. 26 (2010) 608.

[31] S.B. Hocevar, J. Wang, K.P. Deo, M. Musameh, B. Ogorevc, Electroanalysis 17 (2005) 417.

[32] J. Eric, D. Davies, N. Jabeen, J. Inclusion Phenom. Macrocyclic Chem. 46 (2003) 57.

[33] M. Xu, W. Horsthemke, M. Schell, Electrochim. Acta 38 (1993) 919.

[34] A. Walcarius, Anal. Chim. Acta 384 (1999) 1.

[35] D. Gligor, F. Balaj, A. Maicaneanu, R. Gropeanu, I. Grosu, L. Muresan, I.C. Popescu, Mater. Chem. Phys. 113 (2009) 283.

[36] M. Noroozifar, M. Khorasani-Motlagh, P. Ahmadzadeh Fard. J. Hazard. Mater. 166 (2009) 1060.

[37] M. Noroozifar, M. Khorasani-Motlagh, M.N. Gorgij, H.R. Naderpour, J. Hazard. Mater. 155 (2008) 566.

[38] R.L. McCreery, Chem. Rev. 108 (2008) 2646.

[39] A.P. Brown, F.C. Anson, Anal. Chem. 49 (1977) 1589.

[40] J. Wang, A. Walcarius, J. Electroanal. Chem. 407 (1996) 183.

[41] M.M. Taqui-khan, A.E. Martell, J. Am. Chem. Soc. 89 (1967) 4176.

[42] M.M. Moawad, J. Coord. Chem. 18 (2002) 61.

[43] A. Afkhami, D. Nematollahi, L. Khalafi, M. Rafiee, Int. J. Chem. Kinet. 37 (2005) 17.

[44] I. Toshihiko, S. Nobuhiko, Biosens. Bioelectron. 10 (1995) 435.